

# Modelling Airborne Transmission of COVID-19 in Indoor Spaces Using an Advection–Diffusion–Reaction Equation

Zechariah Lau<sup>1</sup>, Katerina Kaouri<sup>1\*</sup>, Ian M. Griffiths<sup>2</sup>

<sup>1</sup> School of Mathematics, Cardiff University, CF24 4AG,

<sup>2</sup> Mathematical Institute, University of Oxford, OX1 6GG

## Abstract

Due to the rate at which the COVID-19 pandemic is spreading, a model for indoors airborne transmission that is quick to implement is required. We create such a model assuming that the concentration of airborne infectious particles is governed by an advection–diffusion–reaction equation. As schools and universities are intensively discussing how to operate their indoor spaces, we solve the model for an average-sized classroom, assuming only one infectious person at the centre of the room, and quantify the effect of several ventilation settings when the person is breathing or talking, both with and without a face mask. We compare our model both with more complex models and with experimental data, where available, and find good agreement. The framework can be easily applied to any other high-risk location, such as hospitals.

We also generate maps of the Time To Infection (TTI) by airborne transmission in the classroom, for various activities and ventilation levels. We then use the TTI maps to quantify the airborne transmission risk at a given time and make recommendations for the Safe Occupancy Time (SOT), for a chosen risk tolerance level. As expected, we find that the SOT decreases as the ventilation quality decreases. We also establish the recommended “vacancy time” after an activity in the room. For example, to achieve an airborne transmission risk of less than 5%, a classroom with the pre-pandemic ASHRAE recommended ventilation would allow 37-minute lessons followed by 35-minute breaks but if the ventilation is poor, 25-minute lessons should be followed by 166-minute breaks. If ventilation meets the ASHRAE pandemic-updated recommendation, 52-minute lessons and 11-minute breaks are allowed. Our model also uncovers power-law relationships for the concentration in the room as a function of time and particle emission rate and for the TTI as a function of ventilation rate and particle emission rate, which may be used as a fast tool to predict the SOT in a multitude of realistic scenarios. Finally, we show that wearing a face mask of 50% efficiency could increase the SOT by 98% and reduce the vacancy time by up to 55%, depending on the ventilation setting.

---

\*kaourik@cardiff.ac.uk

# 1 Introduction

The COVID-19 pandemic started in December 2019 in Wuhan, China. The SARS-CoV-2 virus quickly spread across the globe causing devastation, with more than sixty million confirmed cases worldwide and almost 1.5 million deaths [1]. COVID-19 is transmitted through virus-carrying respiratory droplets, which are released when an infected person coughs, sneezes, talks or even breathes [2, 3]. Evidence has accumulated that also smaller respiratory droplets which become airborne aerosols can transmit the disease [4]. In July 2020, 239 scientists signed an open letter appealing for the recognition of airborne transmission [5], and in October 2020 the US Centre for Disease Prevention and Control acknowledged airborne transmission and updated their guidelines [6].

Models studying the risk of airborne transmission generally fall into one of two types: those built on the well-mixed room (WMR) assumption and Computational Fluid Dynamics (CFD) models. The WMR assumption is that virus-carrying aerosols are instantaneously evenly distributed throughout the room [7, 8], so everyone in the room is equally likely to be infected, regardless of their position. This assumption greatly simplifies the problem by ignoring the complex effects of the air flow on the airborne particles, so the models can be built in spreadsheets and are quick to run [9]. Models built on the WMR assumption were quickly applied to COVID-19 [10, 11, 12].

Various CFD simulations have also investigated the transport of viral COVID-19 aerosols [13, 14, 15, 16, 17, 18]. Some of these studies focus on the transport in the short term (less than 5 minutes) [13, 14, 15], while others show the build-up of aerosols indoors over an hour [17, 18]. CFD simulations are useful in studying airborne transmission as they can take into account the details of the room size, geometry, the complex turbulent airflow and the size distribution of the aerosols, such as in [14].

However, both WMR and CFD models have drawbacks. The WMR models are too simplistic – they ignore the effects of the room geometry and of the turbulent air flow. On the other end of complexity spectrum, CFD models take a long time to run even for small-sized locations, so they cannot easily be applied to a new location and are not suited for ‘dynamic simulations’. Therefore, in this paper we develop a model based on the advection–diffusion–reaction equation which falls in between, in terms of complexity and user-friendliness. This model provides quick simulations while still taking into account the effect of the turbulent airflow. Even though our model is less detailed than CFD models, we shall show that it is able to reproduce the results of more complex simulations while being able to run quickly on a PC, without the need of a supercomputer. Furthermore, we show how our simple model uncovers power-law relationships for the concentration in the room, which may be used as a fast tool to predict safe occupancy times. The computational simplicity of our model is an asset during the urgent times of this current pandemic, and enables easy application to different locations such as classrooms, healthcare clinics and supermarkets.

In Section 2, we present our model for the movement and accumulation of

the airborne particles indoors, produced by a single presymptomatic or asymptomatic spreader of COVID-19 who is breathing or talking. We assume that the advection–diffusion–reaction equation governs the concentration of the virus. As many countries are currently debating the best way to operate their spaces so as to minimise infection rates during the ongoing second wave of the pandemic, we consider an average classroom. In Section 3.1 we determine the viral concentration in the classroom, for four different ventilation scenarios: very poor ventilation, poor ventilation, a pre-pandemic recommended ventilation and a pandemic-updated recommended ventilation. Then, in Section 3.2 using available estimates of the infectious dose of COVID-19 [14] and a formula for the number of infectious particles inhaled [19], we estimate Time To Infection (TTI) by airborne transmission for a susceptible person. This allows us to determine a safe Safe Occupancy Time (SOT), given a specified tolerance for the airborne transmission risk and a recommended “vacancy time”. We also quantify the reduction in the airborne transmission risk when the infected person wears a mask. We uncover power-law relationships in locations and times where the walls of the room do not play a role in the viral concentration. Such power laws allow for even simpler model predictions that may be implemented in different locations. We summarise our work and draw conclusions on how one could use the model for future planning to tackle the pandemic in Section 4

## 2 Methodology

### 2.1 Governing equation and model assumptions

We study the airborne transmission of COVID-19 in an indoor space by creating a 2D model to study the concentration of airborne infectious particles in a rectangular domain, produced by a breathing or talking infectious person who is presymptomatic or asymptomatic, with and without a face mask.

We assume that the droplets due to breathing and talking are released from the infected person with zero initial velocity. These droplets are then transported via advection due to the airflow in the room and diffusion due to turbulent mixing. We suppose that the advection velocity of the air,  $\vec{v}$  (m/s), is solely controlled by the air-conditioning unit. We assume that the recirculation of air leads to turbulent mixing of the infectious particles, which occurs much more rapidly than molecular diffusion due to Brownian motion [20]. Turbulent diffusion is governed by the isotropic eddy diffusion coefficient,  $K$  (m<sup>2</sup>/s), which describes how quickly particles diffuse with time due to turbulent mixing indoors [20].

From these assumptions, we arrive at the governing equation for the airborne transmission of COVID-19 – the advection–reaction–diffusion equation –

$$\frac{\partial C}{\partial t} = \nabla \cdot (K \nabla C) - \nabla \cdot (\vec{v} C) + S, \quad (1)$$

where  $C$  is the concentration of airborne infectious particles (particles/m<sup>2</sup>),  $\nabla$

is the two-dimensional gradient operator,  $t$  is the time (s) and  $S$  is the sum of sources and sinks of viral particles [21].

As the maximum velocity  $|\vec{v}|$  considered is 0.15m/s which is small compared to the speed of sound (340 m/s) (see Table 1 for typical values), we can assume that the air is an incompressible fluid [22]. Hence, the corresponding mass-conservation equation is

$$\nabla \cdot \vec{v} = 0. \quad (2)$$

Following [23], we model the infected person who is breathing or talking as a continuous point source emitting viral particles at a constant rate of  $R$  particles/s. Thus, an infectious person talking or breathing at position  $(x_0, y_0)$  starting at time  $t = t_0$  is modelled as follows:

$$S_{\text{inf}} = R\delta(x - x_0)\delta(y - y_0)H(t - t_0), \quad (3)$$

where  $\delta(x)$  is the Kronecker delta function and  $H(t)$  is the Heaviside step function.

As  $R$  is still unknown we make the assumption that every airborne respiratory particle produced contains the virus. In other words, the emission rate of airborne virus-carrying particles,  $R$ , is the same as the average emission rate of airborne respiratory particles. We also assume that inhaling and exhaling occur at the same rate, so there is no net source or sink of air from the emitter and receiver of the particles.

We assume there is mechanical ventilation in this indoor space provided by air vents Following [24], we model the ventilation effect as a sink term of uniform strength over the domain,

$$S_{\text{vent}} = -\lambda C, \quad (4)$$

where  $\lambda$  is the air exchange rate of the room, measured in  $\text{s}^{-1}$ . This is an approximation since removal of the air by ventilation occurs at a higher rate near the air vents [25] but our approach still allows us to include the effect of ventilation while retaining its key features and without greatly increasing the mathematical complexity of our model.

Assuming there is only one infectious person, we substitute equations (2), (3) and (4) into the advection–diffusion–reaction equation (1) and obtain the partial differential equation (PDE) we will work with:

$$\frac{\partial C}{\partial t} + \vec{v} \cdot (\nabla C) - K\nabla^2 C = R\delta(x - x_0)\delta(y - y_0)H(t - t_0) - \lambda C. \quad (5)$$

For will further assume that the airflow from the air-conditioning unit is constant and uniform. Therefore,  $\vec{v} = (v, 0)$ , with  $v$  constant. The second wave of the pandemic is currently hitting several countries who were debating whether it is safe to keep schools and universities open for face-to-face teaching and optimal methods of operation. Hence, we decided to simulate an average classroom of dimensions 8m ( $l$ )  $\times$  8m ( $w$ )  $\times$  3m ( $h$ ) – see Figure 1.

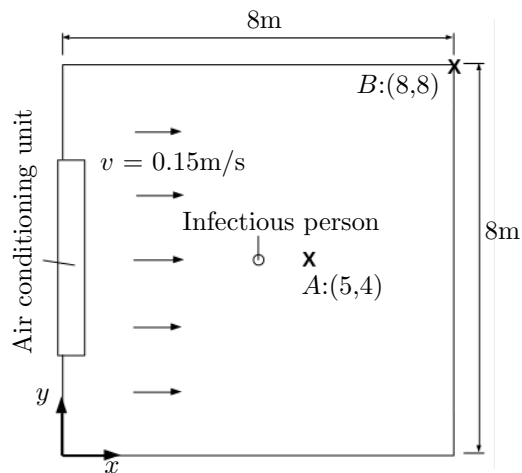


Figure 1: Schematic of the modelled room. One infectious person (viral source) is located at the centre of the room. Positions  $A$  and  $B$  are of particular interest and are studied in our analysis.

We consider four physically relevant ventilation settings which correspond to four different values of  $\lambda$ , the air exchange rate, as follows:

1. Very poor ventilation.
2. Poor ventilation.
3. A pre-pandemic recommended ventilation setting.
4. A pandemic-updated recommended ventilation setting.

For the very poor-ventilation scenario (scenario 1), we take as  $\lambda$  the mean value determined for a closed classroom (closed windows, fans off) with the air conditioning off in a primary school study by [26]. The study investigated the impact of air exchange rates on the indoor pollution particle number concentration and showed that in practice classrooms may have far lower air exchange rates than those recommended. For the poor-ventilation scenario, we take as  $\lambda$  the mean value determined for a closed classroom but now with the air conditioning on [26]. For scenarios 3 and 4, we consider the recommended air exchange rate for classrooms made by the American Society of Heating, Refrigeration and Air-Conditioning Engineers (ASHRAE) before the pandemic [27] and the recommendation they issued for the pandemic [28], respectively.

To determine an approximate value for  $K$ , the eddy diffusion coefficient, we use the following formula, which is valid for an isothermal room served by mixing ventilation. This was developed by [29] and is based on the turbulent kinetic energy balance (TKEB) relationship initially proposed by [30]:

$$K = c_v Q (2c_\epsilon V N^2)^{-1/3}. \quad (6)$$

Here,  $c_v$  is the von Karman constant,  $Q$  is the total volume flow rate into the room,  $V$  is the volume of the room,  $N$  is the number of air supply vents, and  $c_\epsilon$  is the constant of proportionality in Taylor’s Dissipation Law [30, 31]. Since  $Q = V\lambda$ , (6) may be rewritten as

$$K = c_v V \lambda (2c_\epsilon V N^2)^{-1/3}. \quad (7)$$

We assume the relationship  $c_\epsilon = c_v^3$  following [30, 32]. Taking a value  $c_v = 0.39$  [33] gives  $c_\epsilon = 0.059$ . We note, however, that there is some uncertainty about the value of  $c_\epsilon$ . Some applications of the TKEB in the literature have used other formulae for  $c_\epsilon$ , e.g.  $c_\epsilon = c_v$  [24] and  $c_\epsilon = 0.5c_v^3$  [29], without providing a rationale.

We will also quantify the reduction in the airborne transmission risk when the infectious person wears a face mask. The efficiency of surgical masks and N95 respirators is well documented [34]. However, due to the sudden demand produced by the COVID-19 pandemic, there has been a shortage of such masks and many people have had to make do with cloth masks. The efficiency of these masks is not well studied: at the moment there is only a preliminary study by [35], which suggests that the efficiency is at least 50%. Furthermore, a fraction of the general public wear their masks incorrectly, which reduces their efficiency. Thus, we shall assume that a mask has an efficiency of 50% (the worst-case scenario). All parameters and their values are found in Table 1.

## 2.2 Initial and Boundary Conditions

We assume that the initial concentration of infectious aerosols in the room is zero, and that the infected person (the source of infectious particles) is located at the centre of the room. The room walls are modelled as reflecting boundaries, so that no virus particles escape through the walls. The appropriate boundary conditions are then

$$K \frac{\partial C}{\partial x}(0, y, t) - v_x C(0, y, t) = 0 \quad (8a)$$

$$K \frac{\partial C}{\partial x}(l, y, t) - v_x C(l, y, t) = 0 \quad (8b)$$

$$K \frac{\partial C}{\partial y}(x, 0, t) - v_y C(x, 0, t) = 0 \quad (8c)$$

$$K \frac{\partial C}{\partial y}(x, w, t) - v_y C(x, w, t) = 0 \quad (8d)$$

## 2.3 Solving the advection–diffusion–reaction equation

We solve the PDE (5) with the boundary conditions (8) by first solving the homogeneous problem to determine the impulse function. Then, we convolve the impulse with the source function (3) to obtain the full solution [38]. A solution to the homogeneous problem of the form  $\hat{C} = Ae^{-\lambda t}$  is assumed, for some constant  $A$  [38]. We then use the change of variable  $\xi = x - vt$  and

Parameter	Symbol	Value	Source
Rate of production of infectious particles	$R$	Breathing: 0.5 particle/s	[36]
		Talking: 5 particles/s	[36]
		Breathing with mask: 0.25 particles/s	[35]
		Talking with mask: 2.5 particles/s	[35]
Airflow speed	$v$	0.15 m/s	[37]
Length of room	$l$	8m	
Width of room	$w$	8m	
Height of room	$h$	3m	
Room air exchange rate	$\lambda$	Very poor ventilation: $0.12 \text{ h}^{-1} \approx 3.3 \times 10^{-5} \text{ s}^{-1}$	[26]
		Poor ventilation: $0.72 \text{ h}^{-1} \approx 2 \times 10^{-4} \text{ s}^{-1}$	[26]
		Pre-pandemic recommended ventilation: $3 \text{ h}^{-1} \approx 8.3 \times 10^{-4} \text{ s}^{-1}$	[27]
		Pandemic-updated recommended ventilation: $6 \text{ h}^{-1} \approx 1.7 \times 10^{-3} \text{ s}^{-1}$	[28]
von Karman constant	$c_v$	0.39	[33]
Turbulence dissipation constant	$c_\epsilon$	0.059	[30, 32]
Eddy diffusion coefficient	$K$	Very poor ventilation: $8.8 \times 10^{-4} \text{ m}^2/\text{s}$	[29]
		Poor ventilation: $5.3 \times 10^{-3} \text{ m}^2/\text{s}$	[29]
		Pre-pandemic recommended ventilation: $2.2 \times 10^{-2} \text{ m}^2/\text{s}$	[29]
		Pandemic-updated recommended ventilation: $4.4 \times 10^{-2} \text{ m}^2/\text{s}$	[29]

Table 1: Parameter values

separation of variables to reduce to two one-dimensional diffusion problems [38]. Due to the reflecting boundaries, we can use the method of images [25, 39] when solving for the impulse function. Hence, the solution is given by

$$C(x, y, t) = \int_0^t \frac{R}{4\pi K} \sum_{m=-\infty}^{\infty} \left( e^{-\frac{(x-v_x(t-\tau)-x_0-2ml)^2}{4K(t-\tau)}} + e^{-\frac{(x+v_x(t-\tau)+x_0-2ml)^2}{4K(t-\tau)}} \right) \times \sum_{n=-\infty}^{\infty} \left( e^{-\frac{(y-v_y(t-\tau)-y_0-2nb)^2}{4K(t-\tau)}} + e^{-\frac{(y+v_y(t-\tau)+y_0-2nb)^2}{4K(t-\tau)}} \right) \frac{e^{-\lambda(t-\tau)}}{t-\tau} d\tau. \quad (9)$$

We note that  $C$  is proportional to the strength of the source,  $R$ , as expected. Henceforth, we will use the dimensionless parameter  $\mathcal{R} = R/R_0$ , where  $R_0$  is the rate of production of infectious particles when breathing (which is equal to 0.5 particles/s—see Table 1). We choose to work with  $\mathcal{R}$  in all subsequent analysis (see Table 2).

Infectious person state	$R$ (particles/s)	$\mathcal{R} = R/R_0$
Breathing	0.5	1
Talking	5	10
Breathing with mask	0.25	0.5
Talking with mask	2.5	5

Table 2: The rate of production of infectious particles and the corresponding non-dimensional rate when breathing or talking with and without mask, scaled by the production rate during breathing,  $R_0 = 0.5$  particles/s.

## 2.4 Calculating the Time To Infection (TTI) due to airborne transmission

We use the following equation to calculate the number of infectious particles inhaled, adapted from [14] and [19],

$$P(x, y, t) = \int_0^t \rho C(x, y, \tau) d\tau, \quad (10)$$

where  $P$  is the number of infectious particles inhaled and  $\rho$  is the breathing rate, that is, the amount of air inhaled by a person per second, on average.

Since we are modeling exhalation as a continuous process, we also model inhalation as a continuous process. The average person inhales 16 times per minute with an air intake volume of approximately 0.5L [40]. Hence, the breathing rate,  $\rho$  is approximately  $1.3 \times 10^{-4}$  m<sup>3</sup>/s [40].

As we are working in two dimensions, we divide this breathing rate by the height of the turbulent clouds produced by breathing,  $h_c$  [41, 42]. The height of these clouds increases with distance travelled, but a cloud produced by coughing that is at 1m away has a height of about 0.2m [41]. [42] notes that the cross-sectional areas of turbulent jets produced by talking that are at distances greater



than 0.5m ‘envelop the size of a person’s head’, and at a distance of 1.6m a non-negligible concentration contour in the cloud is ‘comparable to the scale of the head’. Based on these observations, we assume the effective  $h_c$  to be the height of a person’s head, which we assume to be 0.2m. This gives  $\rho_{2D} = \rho/h_c = 6.7 \times 10^{-4} \text{ m}^2/\text{s}$ .

To calculate the TTI from (10), we require the infectious dose of COVID-19 particles,  $P_I$ , which is the critical number of airborne particles required to be inhaled for infection to occur. [14] suggests that  $P_I$  for airborne COVID-19 transmission is 100 inhaled particles over three hours, when assuming that the viral load is constant. This estimate is consistent with the infectious dose for SARS-CoV-1 that was estimated to be around 280 particles overnight [43], while [44] compiled a list of the infectious dose of several biological warfare agents which show that bacteria and virus aerosols can cause disease with as few as 1–100 aerosols in two hours. Therefore, this estimate for SARS-CoV-2 of 100 particles is reasonable, keeping in mind that it may have to be updated in the future. This can be easily done in our modelling framework since  $P_I$  is only used in (10) as a threshold figure used for comparison, and nowhere else in our model. Thus, the TTI,  $t_c$ , satisfies the following equation:

$$\int_0^{t_c} \rho_{2D} C(x, y, t) dt = P_I,$$

which we can rearrange to

$$\int_0^{t_c} C(x, y, t) dt = \frac{P_I}{\rho_{2D}} = 1.5 \times 10^5 \text{ particles m}^{-2}\text{s}. \quad (11)$$

Parameter	Symbol	Value	Source
3D breathing rate	$\rho$	$1.3 \times 10^{-4} \text{ m}^3/\text{s}$	[40]
Height of turbulent respiratory cloud	$h_c$	0.2m	[42]
2D breathing rate	$\rho_{2D}$	$6.7 \times 10^{-4} \text{ m}^2/\text{s}$	[40, 42]
Infectious dose	$P_I$	100 particles	[14]

Table 3: Parameter values used in (11) to determine the TTI.

## 2.5 Computations and code: low computational cost

We implement the solution (9) in Python 3.8.5 64-bit. The convolutions are performed using the *convolve* function from the *scipy.signal* subpackage, which convolves two  $N$ -dimensional arrays [45]. To achieve satisfactory accuracy, we used a time step of 0.3s. The infinite series in (9) is evaluated for  $-102 \leq n \leq 102$ . We choose these values of  $n$  because we evaluated the solution for time up to three hours, and during three hours a particle traveling at 0.15m/s reflects off each wall of the room  $3 \times 3600 \times 0.15 / (2 \times 8) = 102$  times.

To determine the TTI, we apply the *cumtrapz* function from the *scipy.integrate* subpackage, which cumulatively integrates an array of values using the trapezoidal rule [45], to the results of the convolutions. The TTI

plots are produced using the Matplotlib library [46]. The TTI contour plots are produced using a rectangular, fine mesh of size 0.05m. The computation time required was approximately four hours for each scenario but it can be reduced using a coarser mesh. We run the simulations on a 2012 MacBook Pro laptop, with a 2.5GHz Dual Core Intel Core i5-3210M processor and 4GB 1805MHz RAM. Our code is available at:  
<https://github.com/zechlau14/Modelling-Airborne-Transmission>.

## 3 Results and discussion

### 3.1 The concentration of airborne infectious particles

Figure 2 shows the concentration of the infectious particles in the room after one hour. In every ventilation scenario, the highest concentration is in the region directly downwind from the infectious person. The width of this region increases with the amount of ventilation, as it depends on the eddy diffusion coefficient,  $K$ , which in turn is proportional to the air exchange rate,  $\lambda$ . The next highest concentration in the room is found upwind, then the concentration decreases as one travels away from the infectious person in the direction orthogonal to the air flow. Our results agree with the results of air sampling in hospital wards in Wuhan, conducted by [47], which showed that virus-carrying particles were ‘mainly concentrated near and downstream from the patients’ and there was also an ‘exposure risk upstream’.

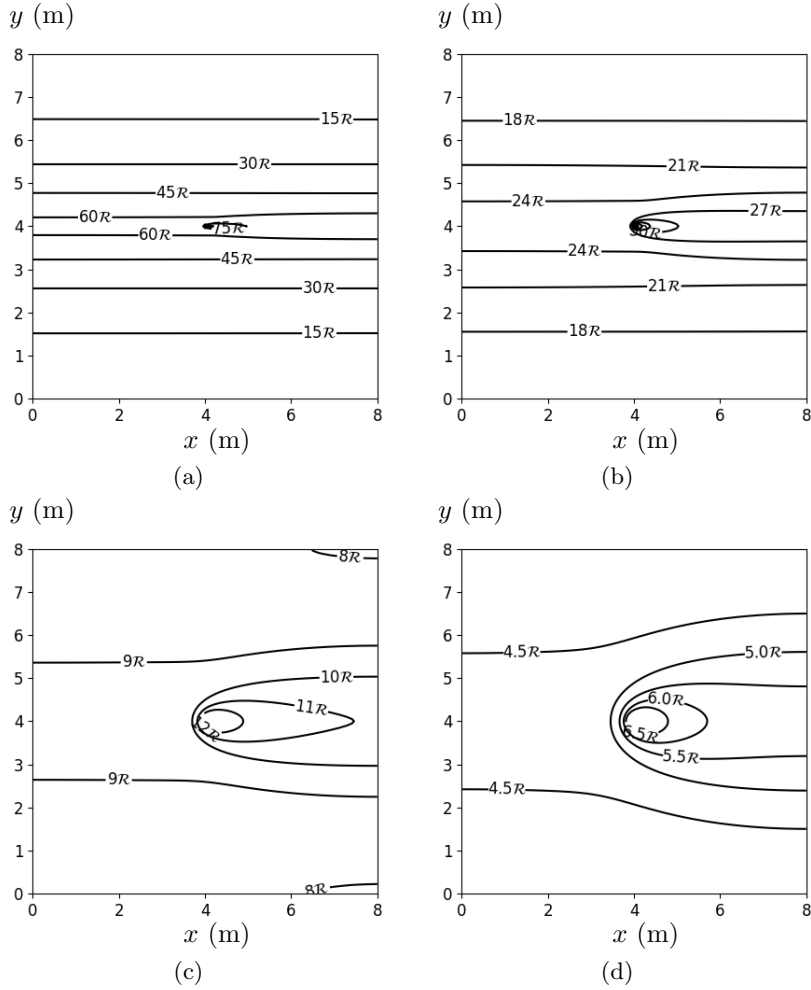


Figure 2: Concentration of viral particles after one hour in a  $8\text{m} \times 8\text{m}$  room, from solving Equation (9): (a) very poor ventilation, (b) poor ventilation, (c) pre-pandemic recommended ventilation, (d) pandemic-updated recommended ventilation. Parameter values are given in Table 1. The innermost contour in each figure corresponds to  $75\mathcal{R}$ ,  $30\mathcal{R}$ ,  $12\mathcal{R}$  and  $6.5\mathcal{R}$  respectively.

Figure 3 shows the concentration in the room versus time evaluated at Position  $A:(5,4)$ , and Position  $B:(8,8)$  (see Figure 1). These two positions were chosen because, as seen in Figure 2, Position  $A$  is where the highest concentration is while maintaining 1m social distancing from the infectious person and Position  $B$  is where the lowest concentration in the room is.

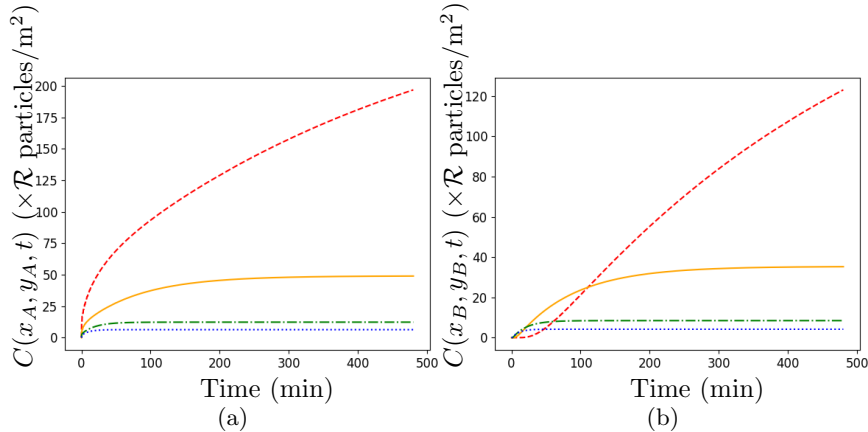


Figure 3: Concentration of particles versus time in a case of very poor ventilation (red dashed), poor ventilation (orange solid), pre-pandemic recommended ventilation (green dot-dashed) and pandemic-updated recommended ventilation (blue dotted), obtained solving Equation (9), with parameter values as given in Table 1. (a) Evaluated at Position A: (5,4). In this case, a power law of the form  $C(x_A, y_A, t) \propto \mathcal{R} t^\alpha$  is obeyed, where  $\alpha = 0.38$ ; the trend deviates from this power law when  $t \approx 20$  minutes since the presence of the walls influences the solution more. (b) Evaluated at Position B: (8,8). In this case, the influence from the walls is significant and hence no scaling law is obeyed.

Figure 3 shows that the concentration increases initially. Then the concentration in the three better-ventilation scenarios will reach steady states, where the rate of change of the concentration falls below  $0.01\mathcal{R}$  particles/m<sup>2</sup> per minute. The very poor-ventilation scenario will also approach a steady state eventually (not shown on this figure).

Figure 3 shows that the lower the value of  $\lambda$ , the greater the time required to approach the steady-state concentration. For the pandemic-updated recommended ventilation, the concentration in the room reaches a steady state ranging from  $4.09\mathcal{R}$  (at Position B) to  $6.23\mathcal{R}$  (at Position A) particles/m<sup>2</sup> after 38 minutes. For the pre-pandemic recommended ventilation, the concentration in the room reaches a steady state that ranges from  $8.26\mathcal{R}$  (at Position B) to  $12.14\mathcal{R}$  (at Position A) particles/m<sup>2</sup> after 77 minutes. When there is poor ventilation, the room only reaches steady state after 321 minutes (5.35 hours), with the concentration at the steady state ranging from  $34.55$  (at Position B) to  $48.26\mathcal{R}$  (at Position A) particles/m<sup>2</sup>. When there is very poor ventilation, the concentration room will finally reach a steady state after 24 hours at levels ranging from  $200.92\mathcal{R}$  (at Position B) to  $274.76\mathcal{R}$  (at Position A) particles/m<sup>2</sup>.

In the high-concentration regions downwind and upwind from the infectious person, such as Position A, advection dominates and Figure 3a shows that we can obtain a power law of the form  $C(x_A, y_a, t) \propto \mathcal{R} t^\alpha$  is obeyed, where  $\alpha = 0.38$  and is independent of the amount of ventilation; only the constant of proportionality depends on  $\lambda$ . The trend deviates from this power law (moving

away by more than 5%) when  $t \approx 20$  minutes.

For positions that are outside the high-concentration regions, such as Position  $B$ , Figure 3b shows that no scaling law is obeyed, which is due to the influence of the walls. Moreover, we see that the better-ventilation scenarios initially have higher concentrations before being overtaken by the worse-ventilation scenarios. This result occurs because the movement of the infectious particles in the direction orthogonal to the airflow is governed by the eddy diffusion coefficient,  $K$ , which increases with  $\lambda$  in (7). Hence, since the better-ventilation scenarios have higher values of  $K$ , the infectious particles diffuse faster in the  $y$ -direction to begin with. However, given sufficient time, the infectious particles in the worse ventilation scenarios will also reach the farthest points of the room, and the concentration there will eventually surpass that in the better-ventilation scenarios. This result is a first indication that including a minimal amount of ventilation could actually increase the risk of transmission compared to the case of very poor ventilation.

## Comparison with air sampling data

We identified only one paper in the literature that measured the concentration of SARS-CoV-2 in the air while providing the dimensions of the room and the ventilation air exchange rate [48]. In [48] two air samples were obtained in a COVID-19 hospital ward of area  $7\text{m} \times 3.5\text{m}$  and a single patient present. The concentration was measured at the two inlets of the room: one inlet (Position 1) is at the left wall, about 2m from the head of the Patient (the viral source). The other inlet, labelled as Position 2, is at the bottom right corner of the room, about 4.8m from the head of the patient. Also,  $\lambda = 6\text{h}^{-1}$ , which corresponds to the pandemic-updated ventilation setting. Note that a COVID-19 patient admitted to the hospital is also likely to exhibit symptoms such as coughing and sneezing. Nevertheless, our model provides a relatively good agreement with the data in [48], at low computational cost.

As our model determines the concentration of airborne infectious particles, in order to have a valid comparison, the viral load of SARS-CoV-2 in airborne particles,  $\theta$ , is required. [49] has estimated the mean aerosol viral load for breathing, using modelling to combine the size-distribution of exhaled breath microdroplets with viral swab and sputum concentrations as approximation for lung lining liquid, to be approximately  $1.7$  viral copies/ $\text{m}^3$  per breath. If we combine this estimate from [49] with the breathing rate  $\rho_{2D}$  and the breathing particle emission rate  $R$ , we obtain  $\theta = 4.53 \times 10^{-4}$  virus copies/particle. Using this value of  $\theta$ , the comparison of the results of our model and the data from [48] can be found in Table 4. Our model correctly predicts that the concentration at Position 2 in [48] is lower than the concentration at Position 1. However, our model over-predicts the concentration by about 50%. This over-prediction could be due to the difficulties mentioned earlier in the section. Another possible reason for the over-prediction is the height of the respiratory plume,  $h_c$ , we assumed in order to determine  $\rho_{2D}$ . For an asymptomatic patient, we had assumed a plume height of 0.2m. However, a COVID-19 patient may have a

larger plume size, since a sneeze could have plume height of about 0.3m [50]. With a larger plume height, our predictions are a lot closer to the air sample results in [48].

Given the several assumptions we made, our predictions are quite satisfactory. For more accurate results we would need to do full 3D simulations. More air sampling data of COVID-19 aerosols in worse-ventilation settings and with asymptomatic infectious persons is also required in order to validate all the airborne transmission models that have been created, including ours.

	Concentration (viral copies/L)	
	Position 1 in [48]	Position 2 in [48]
Data from [48]	30	16
Our model predictions using plume height 0.2m	44.2	28.1
Our model predictions using plume height 0.3m	29.5	18.7

Table 4: Comparison of our predictions with air sampling data from a hospital ward [48].

### Comparison with CFD Models – recirculation effects

We next compare our results to the results obtained by the CFD models in [16] and [17]. Both of these models studied a superspreader outbreak in a restaurant in Guangzhou, China that occurred on January 23, 2020 [51]. The restaurant was found to have  $\lambda = 0.77 \text{ h}^{-1}$  [16], which is similar to the value of  $\lambda$  we considered in the poor-ventilation scenario. In [16], they found that a ‘contaminated recirculation envelope’ was created in the restaurant. In this recirculation envelope, the air-conditioning jet carried the infectious aerosols to the opposite window, then the jet bent downward and returned at a lower height before finally the contaminated air rose and returned to the air-conditioning unit, repeating the cycle. Our model takes into account this recirculation, but in 2D.

The CFD simulation conducted by [17] showed that in this recirculation envelope, which had a width of 3m, the average concentration after 15 minutes is as high as the concentration directly next to the infected person, while the average concentration in this region after 60 minutes is four times higher.

Our results, as seen in Figure 4a, show that there is a 3m-wide region centred at the infectious person where after 15 minutes the concentration is as high as or even higher than the concentration 0.5m downwind from the infectious person if there was no recirculation in the room (Figure 4b). After an hour, our model shows that the concentration in this region is approximately four times greater (see Figure 2b). Therefore, our results are in agreement.

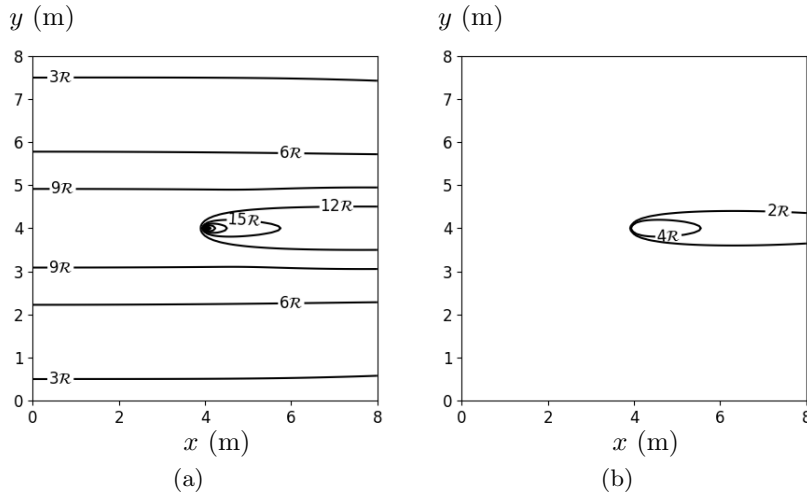


Figure 4: (a) Concentration of particles after 15 minutes in a room with poor ventilation, obtained solving Equation (9), (b) steady-state concentration of viral particles if there is no recirculation, from solving Equation (9) with  $m = n = 0$ . Parameter values are given in Table 1.

### 3.2 Maps of Time to Infection (TTI) by airborne transmission

In this section we construct TTI maps for the four ventilation settings we consider, in an  $8\text{m} \times 8\text{m}$  room. Figure 5 is for very poor ventilation, Figure 6 for poor ventilation, Figure 7 is for pre-pandemic recommended ventilation and Figure 8 is for pandemic-updated recommended ventilation.

As the TTI depends on the concentration, Figures 5, 6, 7 and 8 all have similar shapes to Figures 2a, 2b, 2c and 2d respectively. This implies that the greatest risk of airborne transmission indoors is directly downwind from the infectious person, and the risk decreases as we travel away from the source in a direction orthogonal to the airflow.

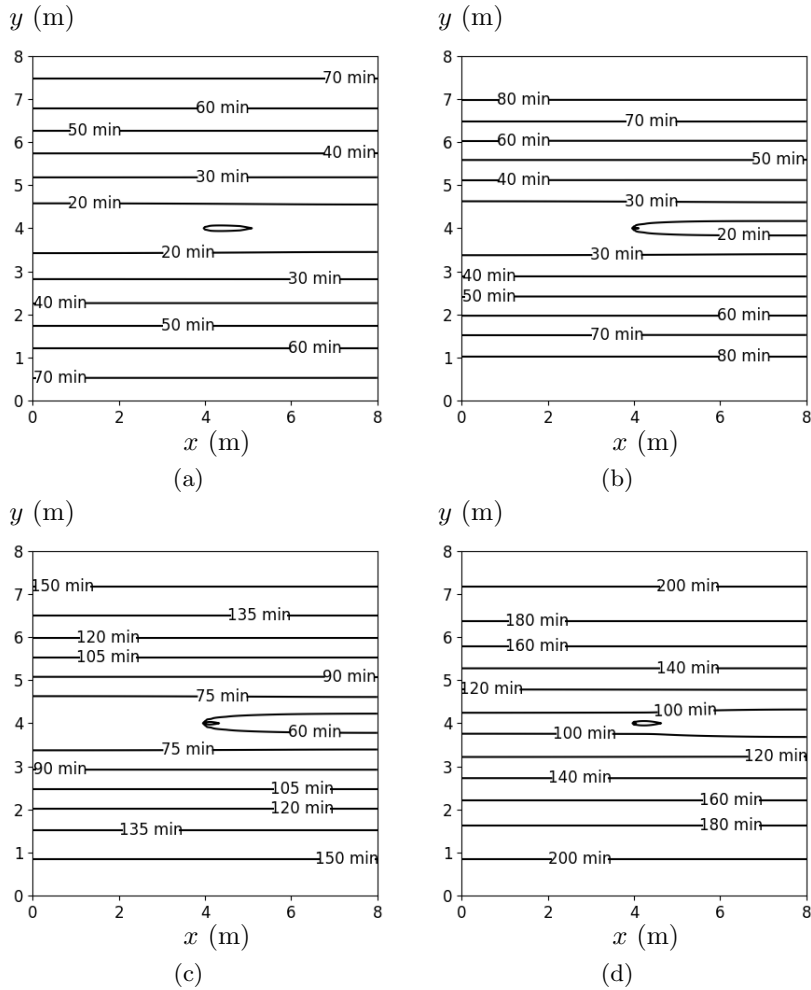


Figure 5: TTI due to an infectious person at the centre of a  $8\text{m} \times 8\text{m}$  room with very poor ventilation, from solving Equations (9) and (11): (a) talking, (b) talking with a mask, (c) breathing, (d) breathing with a mask. Parameter values are given in Table 1. The innermost contour in each figure corresponds to 10 min, 10 min, 45 min and 80 min respectively.



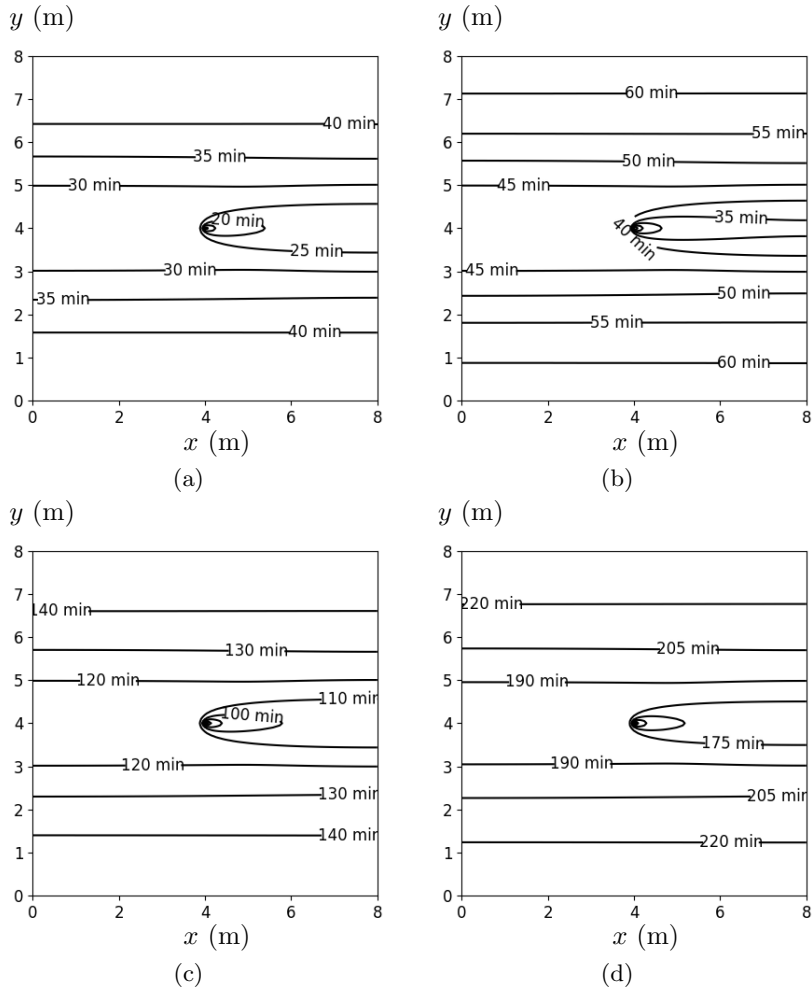


Figure 6: TTI due to an infectious person at the centre of a  $8\text{m} \times 8\text{m}$  room with poor ventilation, from solving Equations (9) and (11): (a) talking, (b) talking with a mask, (c) breathing, (d) breathing with a mask. Parameter values are given in Table 1. The innermost contour in each figure corresponds to 15 min, 30 min, 90 min and 160 min respectively.

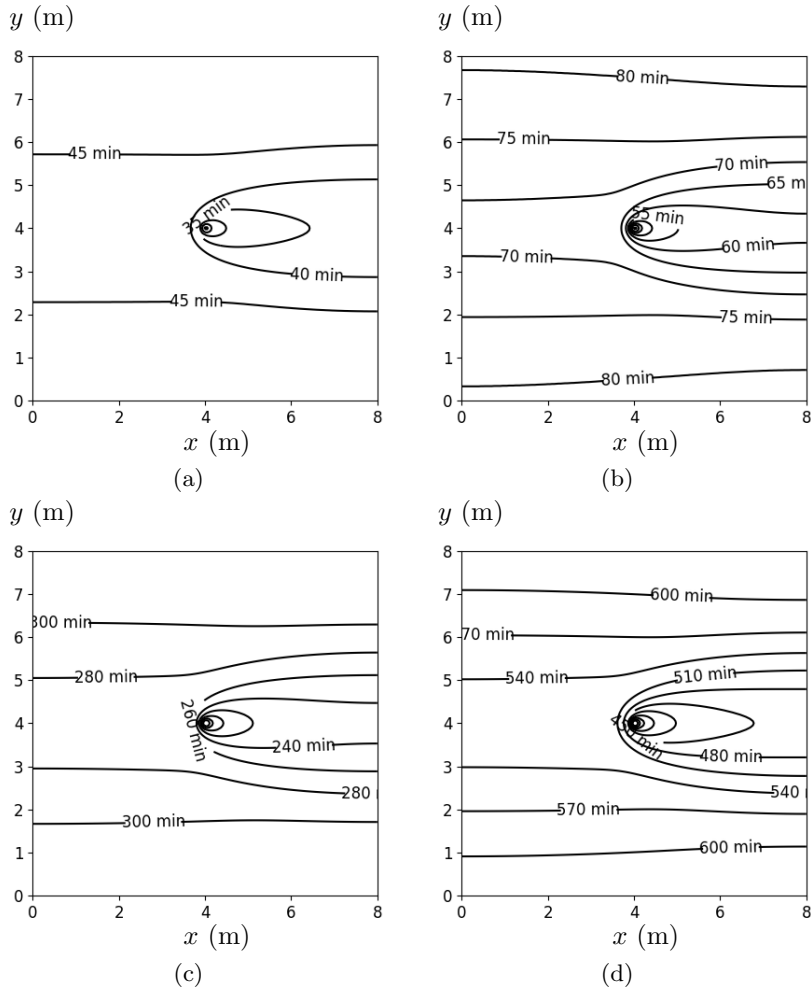


Figure 7: TTI due to an infectious person at the centre of a  $8\text{m} \times 8\text{m}$  room with the pre-pandemic recommended ventilation, from solving Equations (9) and (11): (a) talking, (b) talking with a mask, (c) breathing, (d) breathing with a mask. Parameter values are given in Table 1. The innermost contour in each figure corresponds to 30 min, 50 min, 280 min and 420 min respectively.

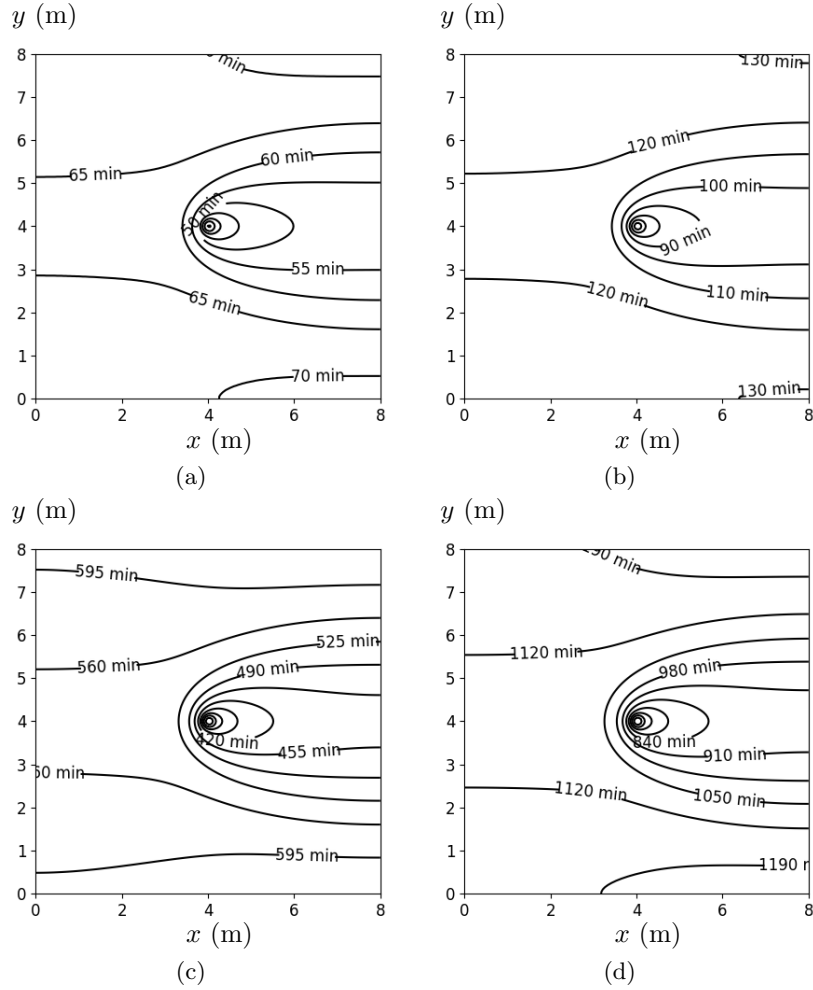


Figure 8: TTI due to an infectious person at the centre of a  $8\text{m} \times 8\text{m}$  room with the pandemic-updated recommended ventilation, from solving Equations (9) and (11): (a) talking, (b) talking with a mask, (c) breathing, (d) breathing with a mask. Parameter values are given in Table 1. The innermost contour in each figure corresponds to 45 min, 80 min, 385 min and 770 min respectively.

From our TTI results, we quantify the risk of airborne transmission in the room at a given time,  $I(t)$ , as follows

$$\begin{aligned}
 I(t) &= \text{Probability(a person is standing at a position with TTI} < t) \\
 &= (\text{fraction of room area where TTI} < t) \times 100\%.
 \end{aligned}
 \tag{12}$$

In this work, we take a risk tolerance of 5% for the  $8\text{m} \times 8\text{m}$  classroom. We choose this tolerance as it corresponds to one new infection in a class of twenty

students, if the Safe Occupancy Time (SOT) is exceeded. Hence if  $I(t) \geq 5\%$ , we will consider the risk of airborne transmission in the room to be *considerable*. This criterion can be easily modified depending on the risk tolerance desired by those operating indoor spaces or imposed by government guidelines.

If the room has very poor ventilation, Figure 5 shows that the TTI is within three hours, which we assume is a reasonable duration for a social gathering, for all the values of  $R$  studied. Therefore, given sufficient time in this room, the risk of airborne transmission becomes considerable.

When there is poor ventilation, Figure 6 shows that without a mask the risk of airborne transmission will become considerable with time. In the aforementioned Guangzhou restaurant super-spreader outbreak, which is similar to our poor-ventilation scenario, the person believed to be the source of the outbreak was in the restaurant for 1 hour and 20 minutes, the infected diners downwind shared the room for 50 minutes and the infected diners upwind shared the room for 1 hour and 15 minutes [16]. This is in agreement with our results in Figure 6a, which shows that the TTI due to a talking person is 20–25 minutes downwind and 25–45 minutes elsewhere in the room. We also note that if the infectious person wears a mask and remains silent (as in Figure 6d), then the TTI in most of the room is above three hours, and hence the risk of airborne transmission is minimised. Hence, talking should be minimised as much as possible and masks should be worn at all times in closed spaces, as per university guidelines.

If the room has good ventilation, as in Figures 7 and 8, then, provided the infectious person is quiet, the TTI in the room is above three hours and the risk of airborne transmission is minimal. However, good ventilation does not completely eliminate the risk of airborne transmission. If the infectious person speaks for sufficient time, the risk of airborne transmission will become considerable.

At the time of writing, the model most used by the general public to estimate the risk of COVID-19 aerosol transmission was developed by Jimenez [9]. This model is built on the Wells–Riley model [7, 8], which is probabilistic and assumes that the air in the room is instantly well mixed. Using (12), we compare our results with the predictions from their model for a quiet activity using the same room dimensions and ventilation scenarios.

Our TTI results (Figures 5c, 6c, 7c, 8c) suggest that the risk of airborne transmission after an hour is minimal, and the Jimenez model agrees with a predicted infection risk of 0.86%–2.46%. In the case of two hours, for the two better ventilation scenarios, our TTI graphs (Figures 7c and 8c) and the Jimenez model (1.89 and 3.41%) suggest that the risk of airborne transmission is minimal. However, for the very poor- and poor-ventilation cases (Figures 5c and 6c), the risk has become more considerable: the Jimenez model estimates a probability of infection of 10.91% and 7.84%, while our results suggests that the risk is approximately 36% and 15%. Therefore, our results are in agreement over which scenarios are risky. Our model predicted lower risk for the two better-ventilation scenarios than the Jimenez model, and higher risk for the two poor ventilation scenarios than the Jimenez model. This difference arose for two reasons: (1) the Wells–Riley model assumed the room is well mixed, while in

our model the mixing of the air was dependent on the ventilation available and (2) the Wells–Riley model assumes a Poisson distribution for the probability of infection while our model assumes that everyone who inhales the critical dose is infected.

Based on our results, we recommend that institutions enact time limits for the usage of their indoor rooms to minimise the risk of airborne transmission. Each room’s Safe Occupancy Time (SOT) should be decided based on its TTI map, which is dependent on the room’s size, geometry, ventilation and the activity conducted in it. Furthermore, this time limit will depend on the risk tolerance of the institution, whether it has a mandatory face mask policy, and what social distancing guidelines it follows.

Table 5 shows the SOT for the different activities in the  $8\text{m} \times 8\text{m}$  classroom when enacting 1m social distancing at our selected risk tolerance of 5%, i.e.  $I(\text{SOT}) = 5\%$ . These results show that a presentation made by an infectious person carries considerable risk of airborne transmission – the SOT is less than two hours even when the infectious person wears a mask in the best ventilation scenario studied. For a quiet activity, if the ventilation in the classroom is very poor or poor, an SOT of 64 minutes or 110 minutes has to be implemented respectively. On the other hand, if the ventilation in the room is good enough, a quiet activity incurs very little risk of airborne transmission.

In these calculations of the SOT, we assumed that there was only one infectious person in the room. In order for the SOT to be effective, we recommend that the occupancy limit of the room not be solely dependent on the social distancing guidelines, but it should also take into account the prevalence of COVID-19 cases in the local community.

Ventilation Scenario	Presentation		Quiet Activity	
	No mask	With mask	No mask	With mask
Very poor ventilation	16 min	24 min	64 min	100 min
Poor ventilation	25 min	39 min	110 min	176 min
Pre-pandemic recommendation	37 min	61 min	240 min(*)	462 min(*)
Pandemic-updated recommendation	52 min	96 min	447 min(*)	885 min(*)

Table 5: The Safe Occupancy Time (SOT) for different activities in an  $8\text{m} \times 8\text{m}$  room if 1m of social distancing is observed for a risk tolerance of 5%, from solving Equation (12) using the TTI data. The results marked with (\*) have times that exceed three hours, which we deem corresponds to minimal risk of airborne transmission.

We note that these SOTs are valid only when the air in the room is free of airborne infectious particles. Therefore, we recommend after each use of the room that the room is left vacant with the ventilation system running so that the air may be refreshed, and the room may be used to its full SOT without concern. We can calculate the vacancy time required by modifying the source

function (3) to a rectangular function ending at the SOT, i.e.

$$S = \begin{cases} R\delta(x - x_0)\delta(y - y_0) & \text{if } t < \text{SOT} \\ = 0 & \text{otherwise} \end{cases} \quad (13)$$

We will consider the air of the room as clean if the concentration of airborne particles is below 13.8 particles/m<sup>2</sup> as clean. We choose this threshold because if the concentration in the room remains below this level the TTI in the room will be greater than three hours. At this concentration, the SOT presented in Table 5 for presentations is not increased by much (less than 5 minutes), so the same SOT can be observed with a small increase in risk. However, as the concentration in the room is much lower when the infectious person is quiet, if the room has the threshold level of concentration, the TTI can fall by as much as 20–40 minutes, so the SOT needs to be recalculated.

In Table 6, we present the vacancy time required to clean the air after each SOT has been reached. Table 6 shows that the vacancy time increases when the ventilation is worse, as expected. We note that, if the classroom has the ASHRAE pre-pandemic recommended ventilation, these vacancy times together with the SOT suggest that the scheduling should be 37-minute lessons followed by 35-minute vacancy times. If the classroom has the pandemic-updated recommended ventilation, then the scheduling can be 52-minute lessons followed by 11-minute vacancy times. For quiet activities in classrooms with good ventilation, the concentration at steady state is low enough that we consider the air in the room clean and there is no need to leave the room vacant. However, if the classroom has poor ventilation, then the required scheduling becomes 25-minute lessons followed by 166-minute vacancy times.

Our results show that wearing a face mask reduces the risk of airborne transmission, as expected. When a mask is worn, the SOT in the room increases (see Table 5), and the required vacancy time decreases (see Table 6). Hence, the recommended scheduling for a classroom with pre-pandemic recommended ventilation becomes 61-minute lessons followed by 23-minute vacancy times, and if it has the pandemic-updated recommended ventilation it becomes 96-minute lessons followed by 5-minute vacancy times. If the ventilation in the classroom is poor, then the recommended scheduling is 39-minute lessons followed by 138-minute vacancy times.

Ventilation Scenario	Presentation		Quiet Activity	
	No mask	With mask	No mask	With mask
Very poor ventilation	846 min	697 min	360 min	218 min
Poor ventilation	166 min	138 min	60 min	18 min
Pre-pandemic recommendation	35 min	23 min	0 min	0 min
Pandemic-updated recommendation	11 min	5 min	0 min	0 min

Table 6: The required vacancy time to refresh the air after different activities in an  $8\text{m} \times 8\text{m}$  room where the SOT is observed, obtained solving Equation (9), for the four ventilation scenarios we consider and for the infected person wearing a face mask or not. Parameters are as in Table 1.

Figures 9 and 10 show the relationship between the TTI and  $\lambda$  at Positions *A* and *B* respectively. In Figure 9 we observe further evidence of the scaling-law behaviour at Position *A* that was identified in Figure 3, by now finding that the TTI satisfies the relationship  $\text{TTI} \propto \lambda^\beta$ , where  $\beta = 0.37$  for  $\lambda < 1\text{h}^{-1}$ , and a linear relationship, i.e.  $\beta = 1$ , for  $\lambda > 1\text{h}^{-1}$ .

Outside the high-concentration region downwind and upwind, such as at Position *B*, Figure 10 shows us that when  $\lambda$  is large, the risk of airborne transmission decreases. However, the TTI also increases as  $\lambda \rightarrow 0$ . This is due to the slower initial build-up of concentration as seen in Figure 3b. Crucially, this non-monotonic behaviour demonstrates that very low ventilation increases the risk of airborne transmission in the area of the room downwind and upwind from the source but decreases the risk everywhere else. This supports the initial observation made in Figure 3.

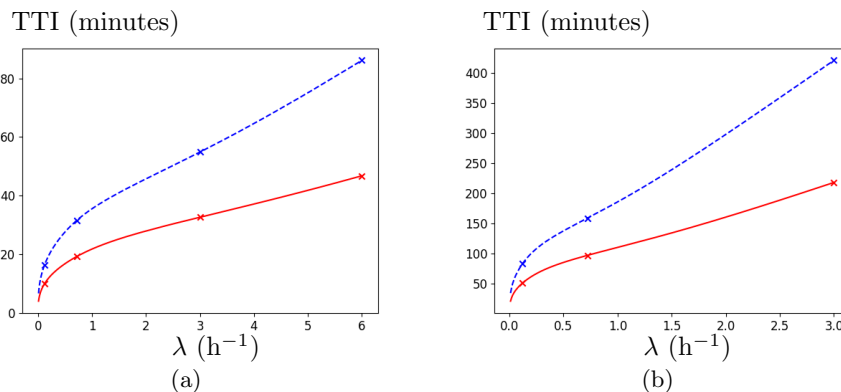


Figure 9: TTI versus the air exchange rate,  $\lambda$ , evaluated at Position *A*, from solving Equations (9) and (11): (a) talking (b) breathing. Red solid line: No mask; Blue dashed line: Wearing a mask. All other parameter values are given in Table 1.

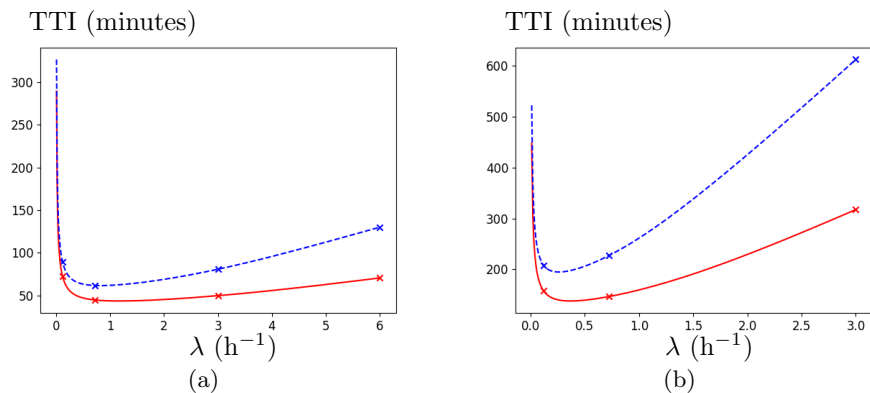


Figure 10: TTI versus the air exchange rate,  $\lambda$ , evaluated at Position  $B$ , from solving Equations (9) and (11): (a) talking (b) breathing. Red solid line: No mask; Blue dashed line: Wearing a mask. All other parameter values are given in Table 1.

Finally, we consider the relationship between the TTI and  $R$ , the emission rate of airborne infectious particles, more closely, as well as the effect of the room's area on the TTI. We consider several other rooms that can also be found in schools and universities: a personal office ( $4\text{m} \times 4\text{m}$ ), an auditorium or lecture theatre ( $30\text{m} \times 15\text{m}$ ), and a convention centre or indoor football field ( $105\text{m} \times 68\text{m}$ ). Figure 11 shows that there is a power law of the form  $\text{TTI} \propto R^\gamma$ . For the  $8\text{m} \times 8\text{m}$  classroom we consider,  $\gamma = -0.71$ . We note that as the size of the room increases to infinity,  $\gamma \rightarrow -1$ . This result provides the specific relationship for how the TTI decreases as  $R$  increases. Furthermore, since  $\gamma$  decreases with increasing room size, this shows that the dependence of the TTI on  $R$  becomes weaker with increasing room size.



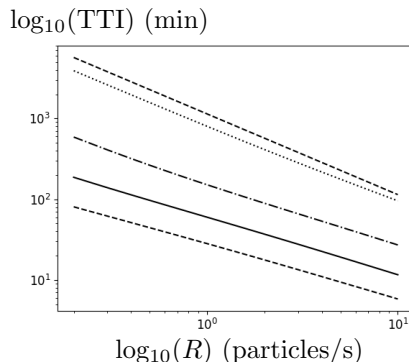


Figure 11: Log–log plot of TTI versus the rate of particle emission,  $R$ , in rooms with poor ventilation, evaluated at 1m downwind from the infectious person, from solving Equations (9) and (11). From top to bottom: the top dashed line represents an infinite room; the dotted line represents a convention centre ( $105\text{m} \times 68\text{m}$ ); the dot-dashed line represents an auditorium ( $30\text{m} \times 15\text{m}$ ); the solid line represents a classroom ( $8\text{m} \times 8\text{m}$ ); and the bottom dashed line represents a personal office ( $4\text{m} \times 4\text{m}$ ). All other parameter values are given in Table 1.

## 4 Summary and conclusions

In this paper, we have addressed the need to develop a quick and efficient model to determine the concentration of airborne particles carrying the SARS-CoV-2 virus in various typical environment settings that takes into account the turbulent airflow. Our model is based on the advection–diffusion–reaction equation. We applied the model to an  $8\text{m} \times 8\text{m}$  room, which represents an average classroom. Then we used the results, an estimated infectious dose from [14] and a formula for the number of infectious particles inhaled adapted from [14] and [19] to calculate the time to infection (TTI) by airborne transmission of COVID-19 in each scenario.

Our model shows that the concentration in the room increases initially, then reaches a steady state, where the rate of increase of the concentration is less than  $0.01\mathcal{R}$  particles/ $\text{m}^2$  per minute (see Figure 3). The time until this steady state is reached is faster and the steady-state concentration is lower when the air exchange rate,  $\lambda$ , is greater. Furthermore, the concentration, and hence the risk of airborne transmission, in the room is highest downwind and upwind from the infectious person (see Figure 2). In this downwind region, the concentration initially obeys a power law of the form  $C \propto \mathcal{R}t^\alpha$ .

Our results show that the TTI in a room is dependent on the geometry of the room, the ventilation setting, and the activity being conducted. Due to the build-up of infectious airborne particles indoors, depending on the scenario, the TTI may be achieved fairly quickly. For example, an average classroom with the pre-pandemic ASHRAE recommended ventilation, the minimum TTI in the room from a presentation from an infectious person can be reached in as little

as 35 minutes (see Figure 7a). As a result, we recommend that institutions enact time limits for the usage of their indoor rooms so that the risk of airborne transmission in the room is minimised. In order to determine the room’s Safe Occupancy Time (SOT), the TTI results can be used to quantify the risk of airborne transmission at any given time (see (12)) then the SOT can be calculated to match the preferred risk tolerance (see Table 5). We further recommend that the room remain vacant after use with the ventilation system running in order to clean the air in the room (see Table 6).

Our results also show that the infectious person wearing a mask of 50% efficiency increases the SOT in a classroom by as much as 50–98%. The effectiveness of the mask increases with the ventilation available in the room. Therefore, in line with governmental guidelines, we recommend the wearing of masks indoors.

The results from our model also confirm the importance of good ventilation to minimising the risk of airborne transmission of COVID-19. For example, if the ventilation in a classroom is poor, the SOT in the room for a quiet activity is 110 minutes, but if the air exchange rate is increased to meet the ASHRAE pandemic-updated recommended ventilation, the risk of airborne transmission becomes minimal and the SOT increases to 447 minutes (see Table 5). Therefore, in order to maximise the usage of indoor space, we recommend institutions increase the ventilation available as much as possible.

We observe that the TTI obeys the scaling-law behaviour in the form of  $\text{TTI} \propto \lambda^\beta$  in the downwind region (see Figure 9). Outside this high concentration region, the TTI exhibits a non-monotonic relationship with  $\lambda$ : it decreases quickly, then increases (see Figure 10). This demonstrates that very low ventilation increases the risk of airborne transmission in the area downwind and upwind from the infectious person, but decreases the risk of airborne transmission everywhere else.

There is also a power law relation between the TTI and  $R$ , the emission rate of airborne infectious particles, of the form  $\text{TTI} \propto R^\gamma$  (see Figure 11). We note that as the size of the room increases to infinity,  $\gamma \rightarrow -1$ .

In conclusion, the model presented in the paper can be implemented to calculate the TTI for rooms of different sizes under different activities. It can also be implemented to quantify the effectiveness of changing the ventilation available in the room. The modelling framework contains a series of parameters that may easily be adjusted in light of new guidelines on ventilation or evidence on the infectious dose. Most importantly for the current COVID-19 pandemic, it can be implemented quickly on a computing device available to the average person.

## 5 Future work directions

There are a variety of next steps that could be taken with this work. Below, we outline some avenues that would be interesting to explore further.

1. More complex ventilation systems

In our model, we modelled the ventilation system as a global sink of airborne viral particles. The model could be improved by modelling air vents as local sinks. Furthermore, other types of ventilation options could also be considered, such as open windows.

2. More complex room geometries or air velocities

We examined the simple scenario of a square room with uniform air velocity from the AC unit. Another possible direction would be to investigate more complex geometries or more complex air flows. Implementation of this into the model would increase the computational cost.

3. Multiple sources

We modelled only one infectious person. We could extend the model by including multiple infectious people, so the source function would become

$$S = \sum_{i=1}^{N_S} R_i \delta(x - x_i) \delta(y - y_i) H(t - t_i), \quad (14)$$

where  $N_S$  is the number of infectious people,  $R_i$  is their respective particle emission rate, and  $(x_i, y_i)$  and  $t_i$  are their respective positions and start times. As the source function is linear, the overall solution can be obtained by adding the response for each individual source.

4. Symptomatic source

We assumed the infectious person was asymptomatic/presymptomatic so they only released infectious airborne particles by breathing or talking. We can extend our model to a symptomatic COVID-19 patient who also released particles by coughing and sneezing by modifying the source function. For this, we could follow [23] and model a sneeze or cough as an instantaneous point source, i.e.

$$S_{\text{cough}} = A \delta(x - x_0) \delta(y - y_0) \delta(t - t_0), \quad (15)$$

where  $A$  is the number of airborne particles produced by a sneeze or cough. Hence the source function becomes

$$S = \delta(x - x_0) \delta(y - y_0) \left( RH(t - t_0) + \sum_{i=1}^M A_i \delta(t - t_i) \right), \quad (16)$$

where  $M$  is the number of coughs and sneezes.

5. Deactivation and settling factors

We assumed that the virus remains infectious and airborne for the entire time considered. Our model can be extended by including a deactivation and settling factor, which can be modelled as a sink to the concentration

$$S_{\text{inact}} = -\chi C, \quad (17)$$

where  $\chi$  is the deactivation factor.

#### 6. Critical infectious dose

In calculating the TTI, we assumed a critical infectious dose,  $P_I$  particles, which if inhaled would cause the receiver to become infected. In real life, the critical infectious dose varies from person to person due to the strength of each person's immune system. Hence, a median infectious dose – the dose required to infect half the population – is usually considered. The deterministic assumption of a fixed critical dose we did could be replaced with a probabilistic approach to the infectious dose.

#### 7. 3D modelling

With the goal of quick and easy implementation, we built our model in 2D. This model can be extended to 3D without the need for any extra assumptions or parameters beyond those already presented in this paper. The model will be more accurate because we would not have to make assumptions about the height of the turbulent respiratory cloud,  $h_c$ , which we used to convert from 3D to a 2D model in this work. However, it would come with the cost of being more computationally expensive.

## Acknowledgements

KK gratefully acknowledges funding from a Sêr Cymru COVID-19 grant, awarded by the Welsh government. IMG gratefully acknowledges support from the Royal Society via a University Research Fellowship.

## References

- [1] World Health Organisation. WHO coronavirus disease (COVID-19) dashboard. Available at: <https://covid19.who.int/>, 2020. [Accessed: 17 September 2020].
- [2] World Health Organization et al. Modes of transmission of virus causing COVID-19: implications for IPC precaution recommendations: scientific brief, 27 March 2020. Technical report, World Health Organization, 2020.
- [3] Y. Jin, H. Yang, W. Ji, W. Wu, S. Chen, W. Zhang, and G. Duan. Virology, epidemiology, pathogenesis, and control of COVID-19. *Viruses*, 12(4):372, 2020.
- [4] S. Asadi, N. Bouvier, A.S. Wexler, and W.D. Ristenpart. The coronavirus pandemic and aerosols: Does COVID-19 transmit via expiratory particles? *Aerosol Science and Technology*, 54(6):635–638, 2020. PMID: 32308568.
- [5] L. Morawska, D.K. Milton, et al. It is time to address airborne transmission of COVID-19. *Clin Infect Dis*, 6:ciaa939, 2020.
- [6] Centers for Disease Control and Prevention. Scientific brief: SARS-CoV-2 and potential airborne transmission. Available at: <https://www.cdc.gov/>

- coronavirus/2019-ncov/more/scientific-brief-sars-cov-2.html, 2020. [Accessed: 5 November 2020].
- [7] E.C. Riley, G. Murphy, and R.L. Riley. Airborne spread of measles in a suburban elementary school. *American Journal of Epidemiology*, 107(5):421–432, 05 1978.
- [8] W.F. Wells et al. *Airborne Contagion and Air Hygiene. An Ecological Study of Droplet Infections*. Cambridge: Harvard University Press (for The Commonwealth Fund), Mass., USA, 1955.
- [9] J.L. Jimenez. 2020 COVID-19 aerosol transmission estimator. Available at: [https://docs.google.com/spreadsheets/d/16K10QkLD4BjgBd08ePj6ytf-RpPMLJ6aXfg3PrIQBbQ/edit#\\$gid=519189277](https://docs.google.com/spreadsheets/d/16K10QkLD4BjgBd08ePj6ytf-RpPMLJ6aXfg3PrIQBbQ/edit#$gid=519189277), 2020. [Accessed: 5 September 2020].
- [10] H. Dai and B. Zhao. Association of infected probability of COVID-19 with ventilation rates in confined spaces: a Wells-Riley equation based investigation. *medRxiv*, 2020.
- [11] G. Buonanno, L. Stabile, and L. Morawska. Estimation of airborne viral emission: quanta emission rate of SARS-CoV-2 for infection risk assessment. *Environment International*, page 105794, 2020.
- [12] C. Sun and Z. Zhai. The efficacy of social distance and ventilation effectiveness in preventing COVID-19 transmission. *Sustainable Cities and Society*, 62:102390, 2020.
- [13] A.H. Shafaghi, F. Rokhsar Talabazar, A. Koşar, and M. Ghorbani. On the effect of the respiratory droplet generation condition on COVID-19 transmission. *Fluids*, 5(3):113, 2020.
- [14] V. Vuorinen, M. Aarnio, M. Alava, V. Alopaeus, N. Atanasova, M. Auvinen, N. Balasubramanian, H. Bordbar, P. Erästö, R. Grande, et al. Modelling aerosol transport and virus exposure with numerical simulations in relation to SARS-CoV-2 transmission by inhalation indoors. *Safety Science*, 130:104866, 2020.
- [15] Y. Feng, T. Marchal, T. Sperry, and H. Yi. Influence of wind and relative humidity on the social distancing effectiveness to prevent COVID-19 airborne transmission: A numerical study. *Journal of Aerosol Science*, page 105585, 2020.
- [16] Y. Li, H. Qian, J. Hang, X. Chen, L. Hong, P. Liang, J. Li, S. Xiao, J. Wei, L. Liu, and M. Kang. Evidence for probable aerosol transmission of SARS-CoV-2 in a poorly ventilated restaurant. *medRxiv*, 2020.
- [17] B. Birnir and L. Angheluta. The build-up of droplet/aerosols carrying the SARS-CoV-2 Coronavirus, in confined spaces. *medRxiv*, 2020.

- [18] S. Shao, D. Zhou, R. He, J. Li, S. Zou, K. Mallery, S. Kumar, S. Yang, and J. Hong. Risk assessment of airborne transmission of COVID-19 by asymptomatic individuals under different practical settings. *Journal of Aerosol Science*, 151:105661, 2020.
- [19] M. Evans. Avoiding COVID-19: Aerosol guidelines. *arXiv*, 2020.
- [20] M. Nicas. Turbulent eddy diffusion model. In C.B. Keil, T.R. Anthony, and C.E. Simmons, editors, *Mathematical Models for Estimating Occupational Exposure to Chemicals*, pages 53–65, Fairfax, VA, 2009. American Industrial Hygiene Association Press.
- [21] R.B. Bird, W.E. Stewart, and E.N. Lightfoot. *Transport Phenomena*. John Wiley & Sons, Inc., New York, 1960.
- [22] D.J. Acheson. *Elementary Fluid Dynamics*. Clarendon Press, Oxford, 1990.
- [23] M. Khalid, O. Amin, S. Ahmed, B. Shihada, and M-S. Alouini. Modeling of viral aerosol transmission and detection. *IEEE Transactions on Communications*, 68(8):4859–4873, 2020.
- [24] P.J. Drivas, P.A. Valberg, B.L. Murphy, and R. Wilson. Modeling indoor air exposure from short-term point source releases. *Indoor Air*, 6(4):271–277, 1996.
- [25] Y. Shao, S. Ramachandran, S. Arnold, and G. Ramachandran. Turbulent eddy diffusion models in exposure assessment – Determination of the eddy diffusion coefficient. *Journal of Occupational and Environmental Hygiene*, 14(3):195–206, 2017. PMID: 27717291.
- [26] H. Guo, L. Morawska, C. He, and D. Gilbert. Impact of ventilation scenario on air exchange rates and on indoor particle number concentrations in an air-conditioned classroom. *Atmospheric Environment*, 42(4):757–768, 2008.
- [27] ASHRAE Standard. Standard 62-2007 ventilation for acceptable indoor air quality. *American Society of Heating, Refrigerating and Air-Conditioning Engineers, Inc., Atlanta, USA*, 2007.
- [28] ASHRAE. Reopening of schools and universities. Available at: <https://www.ashrae.org/technical-resources/reopening-of-schools-and-universities>, 2020. [Accessed: 29 October 2020].
- [29] T. Foat, J. Drodge, J. Nally, and S. Parker. A relationship for the diffusion coefficient in eddy diffusion based indoor dispersion modelling. *Building and Environment*, 169:106591, 2020.
- [30] E. Karlsson, A. Sjöstedt, and S. Håkansson. Can weak turbulence give high concentrations of carbon dioxide in baby cribs? *Atmospheric Environment*, 28(7):1297–1300, 1994.

- [31] G.I. Taylor. Statistical theory of turbulence iv-diffusion in a turbulent air stream. *Proceedings of the Royal Society of London. Series A-Mathematical and Physical Sciences*, 151(873):465–478, 1935.
- [32] S. Bodin. *A predictive numerical model of the atmospheric boundary layer based on the turbulent energy equation*. PhD thesis, Stockholm University, 1979.
- [33] E.L. Andreas. A new value of the von kármán constant: Implications and implementation. *Journal of Applied Meteorology and Climatology*, 48(5):923–944, 05 2009.
- [34] Y. Li, T. Wong, J. Chung, Y.P. Guo, J.Y. Hu, Y.T. Guan, L. Yao, Q.W. Song, and E. Newton. In vivo protective performance of n95 respirator and surgical facemask. *American Journal of Industrial Medicine*, 49(12):1056–1065, 2006.
- [35] E.P. Fischer, M.C. Fischer, D. Grass, I. Henrion, W.S. Warren, and E. Westman. Low-cost measurement of face mask efficacy for filtering expelled droplets during speech. *Science Advances*, 6(36), 2020.
- [36] S. Asadi, A.S. Wexler, C.D. Cappa, S. Barreda, N.M. Bouvier, and W.D. Ristenpart. Aerosol emission and superemission during human speech increase with voice loudness. *Scientific Reports*, 9(1):1–10, 2019.
- [37] ASHRAE Standard. Standard 55-2010, thermal environmental conditions for human occupancy. *American Society of Heating, Refrigerating and Air Conditioning Engineers*, 2010.
- [38] L.C. Evans. *Partial Differential Equations*. Graduate studies in mathematics, v. 19. American Mathematical Society, Providence, R.I., 1998.
- [39] J. Crank. *The Mathematics of Diffusion*. Oxford University Press, Oxford, 1979.
- [40] S. Hallett, F. Toro, and J.V. Ashurst. Physiology, tidal volume, 2020. [Updated 2020 Jun 1]. In: StatPearls [Internet]. Treasure Island (FL): StatPearls Publishing; 2020 Jan-. Available from: <https://www.ncbi.nlm.nih.gov/books/NBK482502/>.
- [41] L. Bourouiba, E. Dehandschoewercker, and J.W.M. Bush. Violent expiratory events: on coughing and sneezing. *Journal of Fluid Mechanics*, 745:537–563, 2014.
- [42] M. Abkarian, S Mendez, N. Xue, F. Yang, and H.A. Stone. Speech can produce jet-like transport relevant to asymptomatic spreading of virus. *Proceedings of the National Academy of Sciences*, 117(41):25237–25245, 2020.
- [43] T. Watanabe, T.A. Bartrand, M.H. Weir, T. Omura, and C.N. Haas. Development of a dose-response model for SARS coronavirus. *Risk Analysis*, 30(7):1129–1138, 2010.

- [44] D.R. Franz, P.B. Jahrling, A.M. Friedlander, D.J. McClain, D.L. Hoover, W.R. Bryne, J.A. Pavlin, G.W. Christopher, and E.M. Eitzen. Clinical recognition and management of patients exposed to biological warfare agents. *JAMA*, 278(5):399–411, 08 1997.
- [45] P. Virtanen, R. Gommers, T.E. Oliphant, M. Haberland, T. Reddy, D. Cournapeau, E. Burovski, P. Peterson, W. Weckesser, J. Bright, S.J. van der Walt, M. Brett, J. Wilson, K.J. Millman, N. Mayorov, A.R.J. Nelson, E. Jones, R. Kern, E. Larson, C.J. Carey, Í. Polat, Y. Feng, E.W. Moore, J. VanderPlas, D. Laxalde, J. Perktold, R. Cimrman, I. Henriksen, E.A. Quintero, C.R. Harris, A.M. Archibald, A.H. Ribeiro, F. Pedregosa, P. van Mulbregt, and SciPy 1.0 Contributors. SciPy 1.0: Fundamental Algorithms for Scientific Computing in Python. *Nature Methods*, 17:261–272, 2020.
- [46] J.D. Hunter. Matplotlib: A 2d graphics environment. *Computing in Science & Engineering*, 9(3):90–95, 2007.
- [47] Z.D. Guo, Z.Y. Wang, S.F. Zhang, X. Li, L. Li, C. Li, Y. Cui, R.B. Fu, Y.Z. Dong, X.Y. Chi, M.Y. Zhang, K. Liu, C. Cao, B. Liu, K. Zhang, Y.W. Gao, B. Lu, and W. Chen. Aerosol and surface distribution of Severe Acute Respiratory Syndrome Coronavirus 2 in hospital wards, Wuhan, China, 2020. *Emerging Infectious Diseases*, 26(7):1583–1591, July 2020.
- [48] J.A. Lednický, M. Lauzardo, Z.H. Fan, A. Jutla, T.B. Tilly, M. Gangwar, M. Usmani, S.N. Shankar, K. Mohamed, A. Eiguren-Fernandez, C.J. Stephenson, M.M. Alam, M.A. Elbadry, J.C. Loeb, K. Subramaniam, T.B. Waltzek, K. Cherabuddi, J.G. Morris, and C.Y. Wu. Viable SARS-CoV-2 in the air of a hospital room with COVID-19 patients. *International Journal of Infectious Diseases*, 100:476 – 482, 2020.
- [49] M. Riediker and D.H. Tsai. Estimation of viral aerosol emissions from simulated individuals with asymptomatic to moderate coronavirus disease 2019. *JAMA Network Open*, 3(7):e2013807–e2013807, 07 2020.
- [50] J.W. Tang, A.D. Nicolle, C.A. Klettner, J. Pantelic, L. Wang, A.B. Suhaimi, A.Y.L. Tan, G.W.X. Ong, R. Su, C. Sekhar, D.D.W. Cheong, and K.W. Tham. Airflow dynamics of human jets: Sneezing and breathing - potential sources of infectious aerosols. *PLOS ONE*, 8(4):1–7, 04 2013.
- [51] J. Lu, J. Gu, K. Li, C. Xu, W. Su, Z. Lai, D. Zhou, C. Yu, B. Xu, and Z. Yang. COVID-19 outbreak associated with air conditioning in restaurant, Guangzhou, China, 2020. *Emerging Infectious Diseases*, 26(7):1628, 2020.